Dissecting cellular function of fibronectin in osteoarthritic cartilage

Hoolwerff, M. van

Chapter 4

Identification and functional characterization of imbalanced osteoarthritis-associated fibronectin splice variants

Marcella van Hoolwerff[1], Margo Tuerlings[1], Imke J.L. Wijnen[1], H. Eka D. Suchiman[1], Davy Cats[2], Hailiang Mei[2], Rob G.H.H. Nelissen[3], Henrike M.J. van der Linden – van der Zwaag[3], Yolande F.M. Ramos[1], Rodrigo Coutinho de Almeida[1], Ingrid Meulenbelt[1]

[1] Dept. of Biomedical Data Sciences, Section Molecular Epidemiology, Leiden University Medical Center, Leiden, The Netherlands
[2] Sequence Analysis Support Core, Leiden University Medical Center, Leiden, The Netherlands
[3] Dept. of Orthopaedics, Leiden University Medical Center, Leiden, The Netherlands

Rheumatology (Oxford). 2022 May 9:keac272
DOI: 10.1093/rheumatology/keac272

Abstract

Objective. To identify *FN1* transcripts associated with osteoarthritis pathophysiology and investigate the downstream effects of modulating *FN1* expression and relative transcript ratio.

Methods. *FN1* transcriptomic data was obtained from our previously assessed RNA sequencing dataset of lesioned and preserved osteoarthritic cartilage samples from the Research osteoArthritis Articular Cartilage (RAAK) study. Differential transcript expression analysis was performed on all 27 *FN1* transcripts annotated in the Ensembl database. Human primary chondrocytes were transduced with lentiviral particles containing short hairpin RNA (shRNA) targeting full-length *FN1* transcripts or non-targeting shRNA. Subsequently, matrix deposition was induced in our 3D in vitro neo-cartilage model. Effects of changes in the *FN1* transcript ratio on sulfated glycosaminoglycan (sGAG) deposition were investigated by Alcian blue staining and dimethylmethylene blue assay. Moreover, gene expression levels of 17 cartilage-relevant markers were determined by reverse transcription quantitative polymerase chain reaction.

Results. We identified 16 *FN1* transcripts differentially expressed between lesioned and preserved cartilage. *FN1-208*, encoding migration-stimulating factor, was the most significantly differentially expressed protein coding transcript. Down-regulation of full-length *FN1* and a concomitant increased *FN1-208* ratio resulted in decreased sGAG deposition as well as decreased *ACAN* and *COL2A1* and increased *ADAMTS-5*, *ITGB1*, and *ITGB5* gene expression levels.

Conclusion. We show that full-length *FN1* down-regulation and concomitant relative *FN1-208* up-regulation was unbeneficial for deposition of cartilage matrix, likely due to decreased availability of the classical arginine-glycine-aspartate (RGD) integrin-binding site of fibronectin.

Introduction

Currently, osteoarthritis (OA) is the most prevalent degenerative joint disease worldwide, associated with a high societal and economic burden [1]. A general hallmark of OA is the degeneration of articular cartilage [2, 3]. To date, no effective treatment to reverse or slow down the disease is available, except pain relief medication and joint replacement surgery. Therefore, more insight into the underlying pathophysiology of OA is necessary for the development of druggable targets.

In this regard, transcriptome-wide analyses of cartilage have been performed to identify underlying biological mechanisms driving OA [4-6]. Specifically, among the highest expressed and significantly up-regulated genes in affected OA cartilage is *fibronectin* (*FN1*) [4, 6]. *FN1* encodes a high molecular weight, dimeric glycoprotein that in articular cartilage is deposited by chondrocytes and mostly localized in the pericellular matrix directly surrounding the chondrocytes [7]. Fibronectin mediates a wide variety of cellular interactions with the extracellular matrix (ECM) by binding to matrix proteins via multiple binding domains, as well as interactions with chondrocytes via integrins that mediate intracellular signaling. The main integrin-binding domain of fibronectin is the arginine-glycine-aspartate (RGD) motif, which binds multiple integrin heterodimers, including the classic fibronectin receptor integrin α5β1 [8]. Recently, it has been shown that fibronectin-α5β1 adhesion is critical for cartilage regeneration in mice [9]. More recently, our group identified a high-impact mutation in the gelatin-binding domain of *FN1* in an early-onset OA family, resulting in decreased binding capacity of fibronectin to collagen type II [10]. Furthermore, fibronectin can be degraded by proteases and the resulting fibronectin fragments are known to amplify catabolic processes in the articular cartilage [11, 12]. Taken together, these studies show that proper binding of fibronectin to both ECM components and integrins is important for cartilage homeostasis.

The fibronectin gene is known to give rise to 20 different protein coding transcripts by virtue of alternative splicing as well as multiple non-protein coding transcripts [13]. Alternative splicing occurs at three major sites, called extra domain A (EDA), extra domain B (EDB), and variable region (V) [14, 15]. Splicing at the EDA and EDB domains results in inclusion or exclusion of one exon, whereas splicing at the V region can occur at multiple splice sites [14]. This splicing variation provides cells with the capacity to generate large numbers of protein isoforms with different binding properties to precisely alter the ECM composition in a developmental and tissue-specific manner. As a result, each isoform has a unique function in cell-ECM interactions [8]. Among *FN1* splice variants is the intact 70 kDa N-terminus of the full-length protein, also known as migration-stimulating factor (MSF) [16]. MSF includes the heparin- and gelatin-binding domains, but does not have the classical RGD integrin-binding domain. Previously, EDB^+, EDB^-, EDA^- and V^+ transcript variants were shown to be present in multiple joint tissues, while EDA^+ transcript variants were rarely detected [17].

It is still unknown which specific *FN1* transcripts may be involved in the response to a healthy or disease state of cartilage, as well as what the effect of changed *FN1* expression is in OA cartilage. Therefore, we aimed to identify *FN1* transcripts associated with the OA process by assessing our previously published RNA sequencing dataset with paired lesioned and preserved OA cartilage samples [4]. Subsequently, the downstream effects of modulating *FN1* expression and the transcript ratio was investigated in our established human 3D in vitro OA cartilage model.

Materials and Methods

Sample description

Macroscopically lesioned and preserved articular cartilage samples were obtained from patients who underwent joint replacement surgery due to OA in the Research Osteoarthritis and Articular Cartilage (RAAK) study, as described previously [18]. The RAAK study was approved by the medical ethics committee of the Leiden University Medical Center (P08.239/P19.013), and written informed consent was obtained from all participants. In the current study, previously assessed RNA-seq data of 101 cartilage samples were used, of which 35 paired samples between lesioned and preserved (25 knees, 7 hips) [4]. The replication cohort consisted of an additional 10 paired cartilage samples (5 knees, 5 hips). Primary articular chondrocytes obtained from knee replacement surgeries of six participants of the RAAK study were isolated and cultured to perform lentiviral transduction. For all sample characteristics, see **Supplementary Table 1**.

RNA sequencing

Total RNA isolation from articular cartilage, sequencing, and quality control was performed as previously described [4]. Detailed information on the alignment, mapping and filtering is available in the **Supplementary Methods**.

Differential expression analysis and replication

Differential expression analysis was performed between lesioned and preserved OA cartilage samples. Results were validated by means of visualizing exon count data and replicated by means of reverse-transcription quantitative polymerase chain reaction (RT-qPCR). More detailed information is available in the **Supplementary Methods**.

Lentiviral production and cell culture

For knockdown experiments, the pLKO.1-puro vector from the Sigma-Aldrich Mission short hairpin RNA (shRNA) library targeting all full-length protein coding transcripts of *FN1* (TRCN0000286357) and non-targeting control virus particles (SHC002) were kindly provided by Martijn Rabelink (Dept. of Cell & Chemical Biology, Leiden University Medical

Center, Leiden, The Netherlands). Detailed information on the lentiviral production and chondrocyte cell culture and transduction is available in the **Supplementary Methods**. In vitro chondrogenesis was induced as previously described [18]. Neo-cartilage pellets and medium were collected following 3 days of chondrogenesis.

Enzyme-linked immunosorbent assay

Culture medium of neo-cartilage pellets of primary chondrocytes transduced with non-targeting shRNA (control) and *FN1* targeting shRNA was collected following 3 days of chondrogenesis. Fibronectin concentration was determined using the Human Fibronectin Enzyme-linked Immunosorbent assay (ELISA) kit (Thermo Fisher Scientific, Vienna, Austria) according to manufacturer's protocol. The absorbance was measured at 450 nm in a microplate reader (Spectramax iD3, Molecular Devices, San Jose, CAL, USA).

Histology and immunohistochemistry

Neo-cartilage pellets were fixed in 4% formaldehyde overnight and stored in 70% ethanol at 4 °C. Detailed information on histology and immunohistochemistry is available in the **Supplementary Methods**.

RNA isolation and relative gene expression analysis

Two neo-cartilage pellets were pooled in 200 µl Trizol reagent (Thermo Fisher Scientific, Carlsbad, CA, USA) and homogenized using micro pestles. Further details on RNA isolation and gene expression analysis is available in the **Supplementary Methods**. Primer sequences are shown in **Supplementary Table 2**.

Sulfated glycosaminoglycan measurement

The sulfated glycosaminoglycan (sGAG) content in the neo-cartilage pellets was measured with the 1,9-dimethylmethylene blue (DMMB) assay [19]. Pellets were digested with 200 µl papain from papaya (Sigma-Aldrich, Zwijndrecht, The Netherlands) at 60 °C overnight. Shark chondroitin sulfate (Sigma-Aldrich, Zwijndrecht, The Netherlands) was used as a reference standard. The absorbance was measured at 525 and 595 nm in a microplate reader (Spectramax iD3, Molecular Devices, San Jose, CA, USA).

FN1 downstream interactions

To identify potential new *FN1* downstream interactions, Pearson correlations were calculated between *FN1* and the previously reported significantly differentially expressed genes (N = 2,387) [4] in the same lesioned (N = 44) and preserved (N = 57) OA cartilage samples (**Supplementary Table 1D**). Genes with $|r| \geq 0.8$ were analyzed for enrichment in protein-protein interactions with the Search Tool for the Retrieval of Interacting Genes/Proteins (STRING, version 11.0) [20].

Statistical analysis

Statistical analyses were performed using SPSS version 25 (IBM). Data are either shown as mean ± SD or box plots, representing the 25th, 50th and 75th percentiles and whiskers representing the lowest and highest data point lying within 1.5 times the interquartile range. Individual samples are depicted by dots in each box plot. The reported P values of the lentiviral experiments were determined by applying a generalized estimating equations (GEE) to the experimental read-out to adjust for dependencies of the different donors [21]. We followed a linear GEE model, with the read-out data as dependent variable, and group and donor as covariate and exchangeable working matrix: Read-out ~ Group + (1|Donor). P values < 0.05 were considered statistically significant. * P < 0.05, ** P < 0.01, *** P < 0.005.

Data availability

The processed dataset generated and the code to reproduce the differential expression analysis is available on https://git.lumc.nl/mvanhoolwerff/fn1-transcripts.

Results

Characterization of *FN1* transcripts in OA cartilage

To characterize the *FN1* transcripts in cartilage, we used our previously assessed RNA-seq data on 35 paired samples (28 knees, 7 hips) of lesioned and preserved OA cartilage (**Supplementary Table 1A**) [4]. Our in-house pipeline was applied to obtain transcriptomic *FN1* data from the Ensembl database, which has 27 *FN1* transcripts annotated (**Supplementary Figure 1**). To robustly detect the *FN1* transcripts expressed in OA cartilage, a cut-off was applied in the lesioned and preserved cartilage samples separately of an average of ≥ 10 counts per three samples. As a result, 22 transcripts were found to be expressed in cartilage, represented as the mean of normalized counts corrected for transcript length and sequencing depth, as shown in **Table 1**. Notably, the highest expressed protein coding transcripts were full-length transcripts *FN1-211* (base mean counts = 430,585.6; quartile 4), which is EDB$^-$, EDA$^-$, and V$^+$, and *FN1-209* (base mean counts = 120,949.2; quartile 4), which is EDB$^+$, EDA$^-$, and V$^+$. Expression levels of *FN1-211* and *FN1-209* represent 39.4% and 21.4%, respectively of total base mean counts, indicating that these were the main protein coding *FN1* transcripts transcribed in OA cartilage. Moreover, among the top 10 highest expressed transcripts, 2 are classified as retained introns and therefore not protein coding, namely *FN1-227* (base mean counts = 50,673.0; quartile 4), and *FN1-225* (base mean counts = 33,536.1; quartile 3), suggesting that these non-protein coding transcripts may be functional in OA cartilage.

Table 1 | Expression levels of the 22 *FN1* transcripts that were robustly expressed in lesioned and preserved osteoarthritic cartilage samples.

Ensembl ID	Name	Biotype	baseMean	Quartile	EDA	EDB	V
ENST00000443816.5	FN1-211	Protein coding	430585.6	4	No	No	Yes
ENST00000432072.6	FN1-209	Protein coding	234116.5	4	No	Yes	No
ENST00000456923.5	FN1-213	Protein coding	113350	4	No	Yes	Yes
ENST00000356005.8	FN1-204	Protein coding	112854.7	4	No	No	Yes
ENST00000498719.1	FN1-227	Retained intron	50673	4			
ENST00000446046.5	FN1-212	Protein coding	37427.2	3	Yes	No	Yes
ENST00000494446.1	FN1-225	Retained intron	33536.1	3			
ENST00000421182.5	FN1-207	Protein coding	30469	3	No	No	Yes
ENST00000357867.8	FN1-205	Protein coding	23405.6	3	No	No	No
ENST00000426059.1	FN1-208	Protein coding	16523.2	3	No	No	No
ENST00000438981.1	FN1-210	Protein coding	3472.7	2	No	No	Yes
ENST00000461974.1	FN1-215	Retained intron	2163.2	2			
ENST00000492816.6	FN1-224	Retained intron	2028	2			
ENST00000471193.1	FN1-217	Retained intron	903.3	2			
ENST00000460217.1	FN1-214	Retained intron	447.5	2			
ENST00000480024.1	FN1-220	Retained intron	277.2	2			
ENST00000473614.1	FN1-218	Retained intron	155.2	1			
ENST00000496542.1	FN1-226	Retained intron	87.6	1			
ENST00000474036.1	FN1-219	Retained intron	68	1			
ENST00000469569.1	FN1-216	Retained intron	41.5	1			
ENST00000480737.1	FN1-221	Retained intron	38.8	1			
ENST00000490833.5	FN1-223	Processed transcript	8.8	1			

The splice variant of the protein coding transcripts is indicated. baseMean = mean of normalized counts of all samples normalized for transcript length and sequencing depth; Quartile = expression in quartiles, with 1 being the lowest en 4 being the highest; EDA = presence EDA domain; EDB = presence EDB domain; V = presence V region.

Differential expression of *FN1* transcripts between lesioned and preserved OA cartilage

To identify specific *FN1* transcripts associated with the OA process, differential expression analysis was performed on the 22 previously identified expressed *FN1* transcripts in paired lesioned and preserved OA cartilage samples, resulting in 16 significantly up-regulated *FN1* transcripts (false discovery rate (FDR) < 0.05, **Table 2**). The most significantly up-regulated transcript was *FN1-220* (fold change 2.8, FDR 5.8 x 10^{-13}), which is classified as a retained intron, but had relatively low expression levels (base mean counts = 277.2; quartile 2). Notably, the most significant up-regulated protein coding transcript was *FN1-208* (fold change 2.3, FDR 4.9 x 10^{-6}, **Supplementary Figure 2**), which encodes migration-stimulating factor. This truncated fibronectin protein contains the heparin- and gelatin-binding domain of fibronectin, but not the integrin-binding domain, and has been identified as a potent motogenic factor yet has not been previously identified in OA cartilage. To validate the differential expression, we analyzed *FN1* exon count data using DEXSeq, which separates the abundance of exons and parts of exons that are not the same for all transcripts in counting bins. We observed

Table 2 | False discovery rate significantly differentially expressed *FN1* transcripts between lesioned and preserved osteoarthritic cartilage samples.

Ensembl ID	Name	Biotype	Quartile	FC	FDR	EDA	EDB	V
ENST00000480024.1	FN1-220	Retained intron	2	2.8	5.8×10^{-13}			
ENST00000494446.1	FN1-225	Retained intron	3	2.4	4.4×10^{-8}			
ENST00000473614.1	FN1-218	Retained intron	1	2.3	1.7×10^{-7}			
ENST00000492816.6	FN1-224	Retained intron	2	2.4	3.3×10^{-6}			
ENST00000426059.1	FN1-208	Protein coding	3	2.3	4.9×10^{-6}	No	No	No
ENST00000496542.1	FN1-226	Retained intron	1	2.9	5.5×10^{-6}			
ENST00000421182.5	FN1-207	Protein coding	3	2.6	5.4×10^{-4}	No	No	Yes
ENST00000490833.5	FN1-223	Processed transcript	1	2.3	1.1×10^{-3}			
ENST00000460217.1	FN1-214	Retained intron	2	2.2	2.1×10^{-3}			
ENST00000471193.1	FN1-217	Retained intron	2	1.8	2.1×10^{-3}			
ENST00000498719.1	FN1-227	Retained intron	4	2.3	5.2×10^{-3}			
ENST00000469569.1	FN1-216	Retained intron	1	1.7	1.5×10^{-2}			
ENST00000461974.1	FN1-215	Retained intron	2	1.8	1.7×10^{-2}			
ENST00000446046.5	FN1-212	Protein coding	3	2.1	3.0×10^{-2}	Yes	No	Yes
ENST00000356005.8	FN1-204	Protein coding	4	2.0	5.0×10^{-2}	No	No	Yes
ENST00000432072.6	FN1-209	Protein coding	4	2.1	5.0×10^{-2}	No	Yes	No

The splice variant of the protein coding transcripts is indicated. Quartile = expression in quartiles, with 1 being the lowest en 4 being the highest; FC = fold change; FDR = false discovery rate; EDA = presence EDA domain; EDB = presence EDB domain; V = presence V region.

that the exon specific for *FN1-208* was higher expressed in lesioned OA cartilage compared to preserved, consequently validating its differential expression (**Supplementary Figure 3**). To replicate the identified up-regulation of *FN1-208* in lesioned cartilage, we performed RT-qPCR for *FN1-208* in an independent cohort consisting of 10 paired cartilage samples (**Supplementary Table 1B**). The transcript was detected in all samples and showed significant up-regulation (fold change 2.0, $P = 9.2 \times 10^{-3}$, **Supplementary Figure 4**).

To explore whether joint-specific *FN1* transcripts could be identified, we performed stratified analyses for knee (28 pairs) and hip samples (7 pairs). After filtering, we identified 22 transcripts to be robustly expressed in knee OA cartilage samples, while 19 transcripts were robustly expressed in hip samples. This difference could be partly explained by the lower number of hip samples in the analysis. Upon performing differential expression analysis on the knee samples, we identified 16 significantly differentially expressed *FN1* transcripts (**Supplementary Table 3**). In the hip samples, we also identified 16 significantly differentially expressed *FN1* transcripts (**Supplementary Table 4**). Notably, we identified one differentially expressed *FN1* transcript (ENST00000490833.5, *FN1-223*) only present in the knee stratified analysis. However, its expression was very low (basemean 8.8; quartile 1); as a result, it was likely removed in the hip analysis due to the filtering. Furthermore, we identified one transcript (ENST00000357867.8, *FN1-205*) that was only significantly up-regulated in the hip stratified analysis. However, upon closer inspection this transcript was

up-regulated in the knee samples, but with a P value slight more than the cut off value of 0.05, namely 0.051. Consequently, we could not identify joint-specific *FN1* transcripts in OA cartilage.

Effect of modulation of *FN1* and *FN1-208* ratio levels on matrix deposition

Next, we aimed to study downstream effects of observed *FN1* transcript changes, including *FN1-208*, in our established human 3D in vitro neo-cartilage model. Since overall *FN1* expression is inherently high in cartilage, we could not obtain big changes by overexpressing *FN1-208* (**Supplementary Figure 5**); therefore, we aimed to down-regulate full-length *FN1*. To this end, primary chondrocytes were lentivirally transduced with *FN1* targeting shRNA, as depicted in **Figure 1A**. The shRNA targets all full-length protein coding *FN1* transcript but not *FN1-208*. Human primary chondrocytes of six donors were transduced (**Supplementary Table 1C**), after which in vitro chondrogenesis was induced in 3D pellet culture for 3 days. Consequently, we observed a down-regulation of the full-length transcripts (*FN1*¸ fold change 0.3, P = 7.6 x 10^{-7}), but since *FN1-208* is not targeted, the *FN1-208* expression relative to full-length transcripts was increased (fold change 3.5, P = 6.0 x 10^{-6}) (**Figure 1B**), thereby mimicking lesioned OA cartilage status. The overall down-regulation of fibronectin was also observed at protein level, both in the neo-cartilage pellets (**Figure 1C**) and culture medium

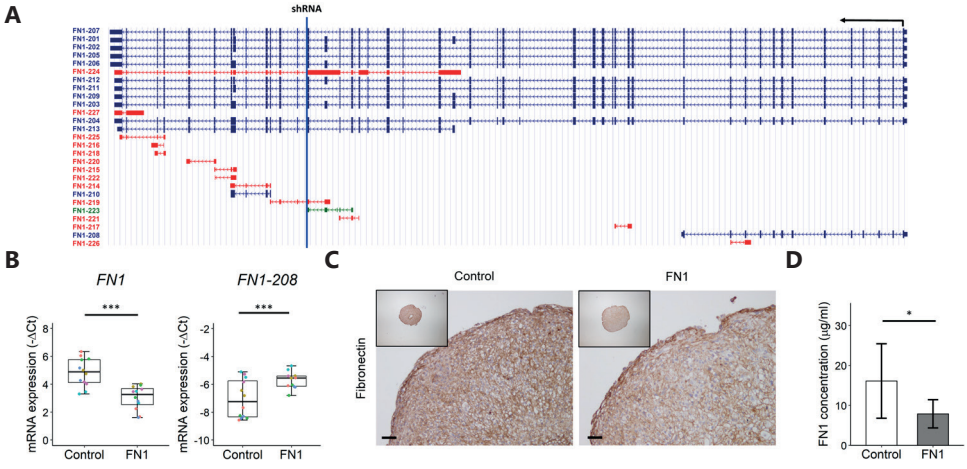

Figure 1 | Down-regulation of *FN1* gene and protein expression in neo-cartilage pellets after 3 days of chondrogenesis. (**A**) Schematic representation of *FN1* transcripts, which are transcribed from the antisense strand, represented by the black arrow. The blue line represents the location of the target sequence of the shRNA targeting *FN1* transcripts. Blue transcripts are protein coding, red and green transcripts are non-protein coding Source: https://genome.ucsc.edu/ (**B**) Gene expression levels depicted by box plots of -ΔCt values of *FN1* and *FN1-208* ratio relative to all full-length *FN1* transcripts in neo-cartilage pellets of primary chondrocytes transduced with non-targeting shRNA (control) and *FN1* targeting shRNA (FN1). Individual samples are represented by colored dots; colors of dots represent the different donors (N = 12) (**C**) Representative images of fibronectin staining of control and *FN1* down-regulated pellets, confirming *FN1* down-regulation on protein level. Scale bar, 50 µm. (**D**) Fibronectin concentration in conditioned medium in the control (N=6) and FN1 group (N=5), as determined by ELISA. Data are means ± SD. P values were determined by GEE, with experimental read-out as dependent variable, and donor and group as covariate. * P < 0.05, *** P < 0.005.

(**Figure 1D**). The fibronectin concentration was 50% decreased in the FN1 group (P = 1.0 x 10^{-2}) compared to the control group, as determined by ELISA.

Subsequently, the effect of *FN1* down-regulation on neo-cartilage deposition was investigated by Alcian blue staining, where we observed a decreased deposition of sGAGs in the *FN1* down-regulated pellets (**Figure 2A**). Quantification of the Alcian blue staining showed that this decreased matrix deposition was 54% (P = 1.3 x 10^{-9}) (**Figure 2B**). Furthermore, quantification of sGAG content normalized to DNA with the DMMB assay confirmed there was a significant decrease (P = 2.6x10^{-2}) in the *FN1* down-regulated group compared with the controls (**Figure 2C**). These data imply that *FN1* down-regulation and concomitant relative up-regulation of *FN1-208* have a negative effect on neo-cartilage deposition.

To investigate the effect of changes in *FN1* transcript ratios on gene expression, RT-qPCR was performed on 17 cartilage-relevant genes (**Supplementary Table 5**). As shown in **Figure 3**, both *ACAN* (fold change 0.5, P = 5.7 x 10^{-3}) and *COL2A1* (fold change 0.1, P = 7.0 x 10^{-7}) were strongly down-regulated in the FN1 group compared with controls. Moreover, *ADAMTS-5* was significantly up-regulated (fold change 2.6, P = 9.0 x 10^{-6}), while *MMP-3* was significantly down-regulated (fold change 0.4, P = 2.9 x 10^{-2}). These data imply that decreased *FN1* expression results in a more catabolic response of the chondrocytes via *ADAMTS-5*.

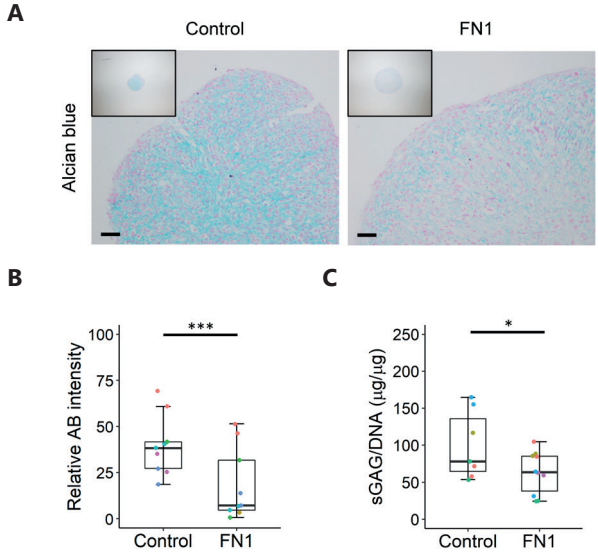

Figure 2 | Decreased overall *FN1* expression and change of *FN1* transcript ratios results in decreased matrix deposition. (**A**) Representative images of Alcian blue staining of neo-cartilage pellets of primary chondrocytes transduced with non-targeting shRNA (control) and *FN1* targeting shRNA (FN1). (**B**) Quantification of Alcian blue (AB) pixel intensity staining of control and *FN1* targeting shRNA transduced pellets (N = 9). Colors of dots represent the different donors. (**C**) sGAG content normalized to DNA content in pellets of the control (N = 7) and FN1 group (N = 11) analyzed by dimethylmethylene blue assay. P values were determined by GEE, with experimental read-out as dependent variable, and donor and group as covariate. * P < 0.05, *** P < 0.005.

Subsequently, we aimed to investigate the downstream effects of *FN1* down-regulation on the fibronectin-binding chondrocyte transmembrane integrin receptors. Gene expression levels of *ITGB1* (fold change 2.2, P = 1.7 x 10^{-4}), and *ITGB5* (fold change 2.9, P = 1.9 x 10^{-4}) were significantly up-regulated in the FN1 group compared with controls (**Figure 3**).

Finally, we aimed to identify novel *FN1* downstream pathways in OA cartilage. To this end, we calculated correlations between our previously reported differentially expressed genes (N = 2,378) and *FN1* in lesioned and preserved OA cartilage (N = 101) samples (**Supplementary Table 1D**) [4]. As a result, we found 60 genes to be highly correlated (|r| > 0.7) (**Supplementary Table 6**). Pathway enrichment analysis between these highly correlating genes (|r>| 0.7) and *FN1* using STRING resulted in five FDR significantly enriched Gene Ontology terms: cell surface (GO:0009986), plasma membrane (GO:0005886), membrane (GO:0016020), vesicle (GO:0031982), and intrinsic component of membrane (GO:0031224) (**Supplementary Table 7**). These processes are mainly characterized by *ITGA5*, *NT5E*, *BCAM*, *CD55*, and *CD109,* indicating the relation of fibronectin with basic cellular processes such as cell adhesion and cell growth. Of the 60 highly correlated genes, 10 showed correlations > 0.8. When analyzing for interaction among these 10 genes and *FN1*, 3 genes were either directly or indirectly connected to *FN1*, namely *ANKH*, *NT5E*, and

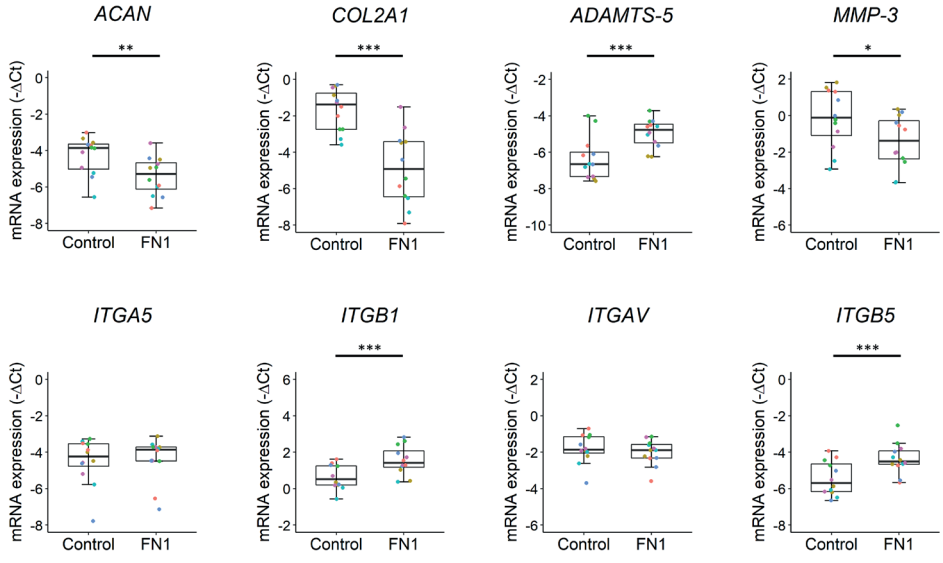

Figure 3 | Decreased *FN1* expression and change of *FN1* transcript ratios results in catabolic chondrocyte metabolism. Box plots of -ΔCt values of cartilage matrix-relevant genes *ACAN*, *COL2A1*, *ADAMTS-5*, *MMP-3*, *ITGA5*, *ITGB1*, *ITGAV*, *ITGB5* in neo-cartilage pellets of primary chondrocytes transduced with non-targeting shRNA (control) (N = 12), and *FN1* targeting shRNA (FN1) (N = 12). Individual samples are represented by colored dots; colors of dots represent the different donors. P values were determined by GEE, with experimental read-out as dependent variable and donor and group as covariate. * P < 0.05, ** P < 0.01, *** P < 0.005.

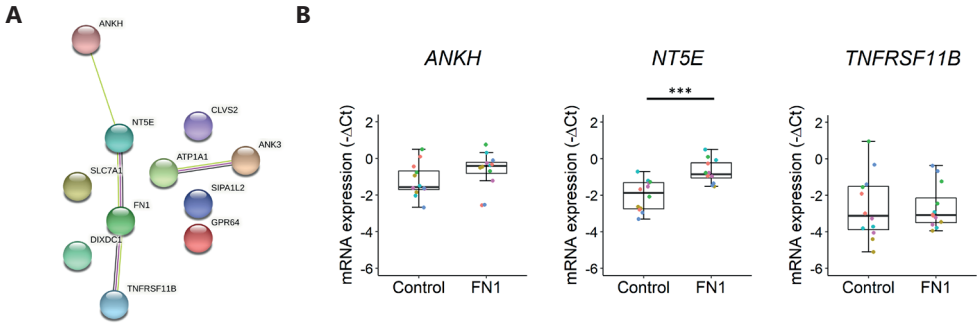

Figure 4 | Identification of new *FN1* downstream genes (**A**) Protein-protein interactions between the genes with correlations |r| > 0.8 with *FN1* in preserved and lesioned OA cartilage samples, as determined with STRING. (**B**) Box plots of -ΔCt values of connected genes to *FN1*, *ANKH*, *NT5E*, and *TNFRSF11B* in neo-cartilage pellets of primary chondrocytes transduced with non-targeting shRNA (control) (N = 12), and *FN1* targeting shRNA (FN1) (N = 12). Individual samples are represented by colored dots; colors of dots represent the different donors. P values were determined by GEE, with experimental read-out as dependent variable and donor and group as covariate. *** P < 0.005.

TNFRSF11B (**Figure 4A**). As shown in **Figure 4B**, only *NT5E* (fold change 2.5, P = 3.0 x 10^{-6}) was significantly differentially expressed in the FN1 group compared with controls.

Discussion

To the best of our knowledge, we are the first to use RNA sequencing to characterize the *FN1* transcriptome in OA cartilage. As a result, we identified 16 *FN1* transcripts FDR significantly up-regulated in lesioned OA cartilage, of which 5 were protein coding and 11 non-protein coding. These results show that considerable changes occur in the *FN1* transcriptome during OA, likely affecting proper function. Moreover, we identified the truncated protein coding transcript *FN1-208* to be significantly up-regulated in lesioned OA cartilage. Upon down-regulation of full-length *FN1* in our human 3D in vitro OA cartilage model, we generated an increased ratio of *FN1-208* relative to the full-length *FN1* transcripts, as such mimicking cartilage in an OA-affected state. This resulted in decreased cartilage deposition compared with the control group, with up-regulation of the β1 and β5 integrin subunits, suggesting a change of integrin heterodimers. Together, our results show that down-regulation of full-length *FN1* is unbeneficial for neo-cartilage deposition, while also highlighting the importance of balance of *FN1* transcripts for healthy cartilage homeostasis.

We identified *FN1-208,* known as MSF, as the most significantly up-regulated protein coding transcript, which has not been previously associated with OA. MSF contains the functional heparin- and gelatin-binding domain of full-length fibronectin and can not bind to transmembrane integrins via the classical RGD binding site. As a result, MSF has distinctive bioactivity compared with full-length fibronectin. MSF has been shown to be a potent motogenic factor and has been associated with cancer pathogenesis as potential driver

of tumor progression by inducing angiogenesis [16, 22]. Furthermore, blocking of MSF suppressed tumor growth through inhibition of tumor-related angiogenesis in an in vitro esophageal cancer model [23]. Angiogenesis contributes to OA pathology, as blood vessels from the subchondral bone invade the articular cartilage, thereby disrupting homeostasis of the chondrocytes. Therefore, we aimed to study whether the identified up-regulation of *FN1-208* is beneficial or unbeneficial to the OA process in cartilage. Since *FN1* is already highly expressed in our established in vitro neo-cartilage model, we could not obtain a significant up-regulation of *FN1-208*. Therefore, we down-regulated full-length *FN1* expression in our model and as a result we obtained an increased *FN1-208* ratio, thus mimicking an OA-related up-regulation. Consequently, in our study design we cannot distinguish between the effect of down-regulating *FN1* and increasing relative amounts of the OA-sensitive transcript *FN1-208*. Nonetheless, the shift in *FN1-208* ratio relative to the total protein coding transcripts resulted in a decreased neo-cartilage deposition, as well as a catabolic state of the chondrocytes. Moreover, we observed up-regulation of *ITGB1* and *ITGB5* gene expression levels. It has been shown that the β1 integrin is up-regulated in osteoarthritic compared to normal cartilage [24]. Therefore, the up-regulation of *ITGB1* and *ITGB5* may represent a higher disease state of the chondrocytes in the *FN1* down-regulated pellets. Together, these data show that decreased availability of the classical integrin-binding site of fibronectin to the cells is detrimental for chondrogenesis, which is likely mediated via β1 and β5 integrin subunits. However, this should be confirmed by quantifying protein expression of the integrin subunits, e.g., by Western Blot. Furthermore, investigating changes in integrin-downstream signaling can shed light on the effects of *ITGB1* and *ITGB5* up-regulation.

The retained intron transcripts *FN1-225* and *FN1-227* were relatively highly expressed and significantly differentially expressed between lesioned and preserved OA cartilage, suggesting they may play a role in OA pathophysiology. Intron retention as alternative splicing mechanism has recently been getting more attention regarding potential regulatory functions as opposed to being merely a consequence of mis-splicing [25]. Intron retention is mostly associated with down-regulation of gene expression via nonsense-mediated decay of the intron-retaining transcript, which has been shown to be a physiological mechanism of gene expression control regulating granulocyte differentiation [26]. However, intron retention has been suggested to potentially regulate non-coding RNAs contained within such introns [27]. Future studies regarding the function of retained intron *FN1* transcripts should address whether they regulate gene expression levels of the protein coding *FN1* transcripts, for example via expression or regulation of non-coding RNAs, such as micro-RNAs or long non-coding RNAs.

Previously, Scanzello *et al.* [17] investigated fibronectin splice variants in joint tissues, including cartilage. EDB^+, EDB^-, and EDA^- variants were found to be present in cartilage, while EDA^+ variants were barely detected, as determined by RT-PCR. In line with these

observations, we identified *FN1-211* and *FN1-209* to be the highest expressed transcripts in OA cartilage, which are both EDA^-. The only EDA^+ transcript that we identified to be robustly expressed in OA cartilage was *FN1-212* (base mean counts = 37,427.2; quartile 3), which represented only 3.4% of the total transcripts. The EDA domain has been associated with many of the functions ascribed to fibronectin, including cell adhesion, matrix assembly, and dimer formation [13, 28]. However, given its low expression, our results suggest that the EDA domain is not essential for proper functioning of fibronectin in cartilage. On a different note, we observed *FN1-213* to be highly expressed (base mean counts =113,350.0; quartile 4), which is a 5'-truncated transcript, that has not been previously identified in cartilage.

All in all, we showed that RNA sequencing is a powerful technique for identifying involvement of the known *FN1* transcripts in OA cartilage. However, the previously identified cartilage specific $(V+III-15+I-10)^-$, $(V+I-10)^-$ and $(V+III-15)^-$ variants were not present in the Ensembl database and were therefore not detected in our analysis [29, 30]. To circumvent this issue, de novo transcriptome assembly could be performed. Nonetheless, in the current study we prioritized reporting previously unknown *FN1* transcripts present in the Ensembl database involved in OA pathophysiology, as opposed to reporting on previously identified *FN1* transcripts. A drawback of our study design is that we only investigated end-stage OA cartilage. Consequently, we cannot identify *FN1* transcripts that are specific for OA cartilage compared to healthy cartilage and thereby potentially be involved in the early phase of OA pathophysiology. Nonetheless, our paired analysis allows for identification of *FN1* transcripts specific to the pathophysiologic process of OA, independent of confounding factors such as sex and age.

To explore potential *FN1* downstream pathways, correlations were calculated between *FN1* and differentially expressed genes in OA cartilage. Among the highest correlated genes, three genes were interconnected in a protein network. Among these three genes, we identified *NT5E* as a novel *FN1* signaling downstream gene in cartilage. *NT5E* encodes the protein 5'-nucleotidase, also known as CD73, which is a plasma protein that catalyzes the conversion of extracellular nucleotides to membrane-permeable nucleosides and is a marker for mesenchymal stromal cells [31]. In addition to the enzymatic function, CD73 also functions as a receptor molecule that can interact with ECM components [32]. Defects in *NT5E* resulting in CD73 deficiency have been shown to facilitate calcification of joints [33, 34], whereas *NT5E* was significantly up-regulated in between lesioned and preserved OA cartilage [4]. These data imply that its up-regulation as a result of *FN1* down-regulation is a compensatory mechanism as a response to the OA disease state.

In conclusion, we identified multiple novel *FN1* transcripts associated with OA pathophysiology, while showing the potential role of *FN1-208*. We show that down-regulation of full-length *FN1*

was unbeneficial for neo-cartilage deposition and resulted in up-regulation of integrin β1 and β5 expression levels, likely via decreased availability of the classical RGD integrin-binding site of fibronectin.

Acknowledgements

We thank all the participants of the RAAK study (supported by Leiden University Medical Center). We thank all the members of the MolEpi Osteoarthritis group for valuable discussion and feedback. We also thank Demiën Broekhuis, Robert van der Wal, Anika Rabelink-Hoogenstraaten, Peter van Schie, Shaho Hasan, Maartje Meijer, Daisy Latijnhouwers and Geert Spierenburg for collecting the RAAK material. We thank Martijn Rabelink for kindly providing us with the lentiviral shRNA plasmids and virus from the Mission shRNA library and performing the lentiviral p24 ELISA. Data is generated within the scope of the Medical Delta programs Regenerative Medicine 4D: Generating complex tissues with stem cells and printing technology and Improving Mobility with Technology.

Funding:

The study was funded by the Dutch Research council/NWO/ZonMW VICI scheme [nr 91816631/528], Dutch Arthritis Society [grant nr DAF-16-1-405].

References

1. Litwic, A., et al., *Epidemiology and burden of osteoarthritis*. Br Med Bull, 2013. **105**: p. 185-99.
2. Loeser, R.F., et al., *Osteoarthritis: a disease of the joint as an organ*. Arthritis Rheum, 2012. **64**(6): p. 1697-707.
3. Goldring, S.R. and M.B. Goldring, *Changes in the osteochondral unit during osteoarthritis: structure, function and cartilage-bone crosstalk*. Nat Rev Rheumatol, 2016. **12**(11): p. 632-644.
4. Coutinho de Almeida, R., et al., *RNA sequencing data integration reveals an miRNA interactome of osteoarthritis cartilage*. Ann Rheum Dis, 2019. **78**(2): p. 270-277.
5. Aki, T., et al., *A whole-genome transcriptome analysis of articular chondrocytes in secondary osteoarthritis of the hip*. PLoS One, 2018. **13**(6): p. e0199734.
6. Ramos, Y.F., et al., *Genes involved in the osteoarthritis process identified through genome wide expression analysis in articular cartilage; the RAAK study*. PLoS One, 2014. **9**(7): p. e103056.
7. Singh, P., C. Carraher, and J.E. Schwarzbauer, *Assembly of fibronectin extracellular matrix*. Annu Rev Cell Dev Biol, 2010. **26**: p. 397-419.
8. Pankov, R. and K.M. Yamada, *Fibronectin at a glance*. J Cell Sci, 2002. **115**(Pt 20): p. 3861-3.
9. Almonte-Becerril, M., et al., *Genetic abrogation of the fibronectin-alpha5beta1 integrin interaction in articular cartilage aggravates osteoarthritis in mice*. PLoS One, 2018. **13**(6): p. e0198559.
10. van Hoolwerff, M., et al., *High-impact FN1 mutation decreases chondrogenic potential and affects cartilage deposition via decreased binding to collagen type II*. Sci Adv, 2021. **7**(45): p. eabg8583.

11. Homandberg, G.A., *Potential regulation of cartilage metabolism in osteoarthritis by fibronectin fragments*. Front Biosci, 1999. **4**: p. D713-30.
12. Reed, K.S.M., et al., *Transcriptional response of human articular chondrocytes treated with fibronectin fragments: an in vitro model of the osteoarthritis phenotype*. Osteoarthritis Cartilage, 2020.
13. White, E.S. and A.F. Muro, *Fibronectin splice variants: understanding their multiple roles in health and disease using engineered mouse models*. IUBMB Life, 2011. **63**(7): p. 538-46.
14. Schwarzbauer, J.E. and D.W. DeSimone, *Fibronectins, their fibrillogenesis, and in vivo functions*. Cold Spring Harb Perspect Biol, 2011. **3**(7).
15. Schwarzbauer, J.E., *Alternative splicing of fibronectin: three variants, three functions*. Bioessays, 1991. **13**(10): p. 527-33.
16. Schor, S.L., et al., *Migration-stimulating factor: a genetically truncated onco-fetal fibronectin isoform expressed by carcinoma and tumor-associated stromal cells*. Cancer Res, 2003. **63**(24): p. 8827-36.
17. Scanzello, C.R., et al., *Fibronectin splice variation in human knee cartilage, meniscus and synovial membrane: observations in osteoarthritic knee*. J Orthop Res, 2015. **33**(4): p. 556-62.
18. Bomer, N., et al., *Underlying molecular mechanisms of DIO2 susceptibility in symptomatic osteoarthritis*. Ann Rheum Dis, 2015. **74**(8): p. 1571-9.
19. Farndale, R.W., D.J. Buttle, and A.J. Barrett, *Improved quantitation and discrimination of sulphated glycosaminoglycans by use of dimethylmethylene blue*. Biochim Biophys Acta, 1986. **883**(2): p. 173-7.
20. Szklarczyk, D., et al., *STRING v11: protein-protein association networks with increased coverage, supporting functional discovery in genome-wide experimental datasets*. Nucleic Acids Res, 2019. **47**(D1): p. D607-D613.
21. Zeger, S.L. and K.Y. Liang, *Longitudinal data analysis for discrete and continuous outcomes*. Biometrics, 1986. **42**(1): p. 121-30.
22. Schor, A.M. and S.L. Schor, *Angiogenesis and tumour progression: migration-stimulating factor as a novel target for clinical intervention*. Eye (Lond), 2010. **24**(3): p. 450-8.
23. Hu, H., et al., *Antibody library-based tumor endothelial cells surface proteomic functional screen reveals migration-stimulating factor as an anti-angiogenic target*. Mol Cell Proteomics, 2009. **8**(4): p. 816-26.
24. Loeser, R.F., C.S. Carlson, and M.P. McGee, *Expression of beta 1 integrins by cultured articular chondrocytes and in osteoarthritic cartilage*. Exp Cell Res, 1995. **217**(2): p. 248-57.
25. Jacob, A.G. and C.W.J. Smith, *Intron retention as a component of regulated gene expression programs*. Hum Genet, 2017. **136**(9): p. 1043-1057.
26. Wong, J.J., et al., *Orchestrated intron retention regulates normal granulocyte differentiation*. Cell, 2013. **154**(3): p. 583-95.
27. Wong, J.J., et al., *Intron retention in mRNA: No longer nonsense: Known and putative roles of intron retention in normal and disease biology*. Bioessays, 2016. **38**(1): p. 41-9.
28. Manabe, R., N. Oh-e, and K. Sekiguchi, *Alternatively spliced EDA segment regulates fibronectin-dependent cell cycle progression and mitogenic signal transduction*. J Biol Chem, 1999. **274**(9): p. 5919-24.
29. Parker, A.E., et al., *Novel cartilage-specific splice variants of fibronectin*. Osteoarthritis Cartilage, 2002. **10**(7): p. 528-34.
30. MacLeod, J.N., et al., *Fibronectin mRNA splice variant in articular cartilage lacks bases encoding the V, III-15, and I-10 protein segments*. J Biol Chem, 1996. **271**(31): p. 18954-60.
31. Dominici, M., et al., *Minimal criteria for defining multipotent mesenchymal stromal cells. The International Society for Cellular Therapy position statement*. Cytotherapy, 2006. **8**(4): p. 315-7.
32. Andrade, C.M., et al., *Ecto-5'-nucleotidase/CD73 knockdown increases cell migration and mRNA level of collagen I in a hepatic stellate cell line*. Cell Tissue Res, 2011. **344**(2): p. 279-86.
33. Ichikawa, N., et al., *Arterial Calcification Due to Deficiency of CD73 (ACDC) As One of Rheumatic Diseases Associated With Periarticular Calcification*. J Clin Rheumatol, 2015. **21**(4): p. 216-20.
34. St Hilaire, C., et al., *NT5E mutations and arterial calcifications*. N Engl J Med, 2011. **364**(5): p. 432-42.

Supplementary Methods

RNA sequencing

Reads were aligned to the GrCh38 reference genome with RNA-seq aligner HISAT2 (version 2.1.0) [1]. Thereafter, aligned reads were processed into individual transcripts using Salmon (version 0.10.1) [2], which were then mapped to Ensembl annotated transcripts (version 97) [3]. Transcript abundance was quantified using the tximport R package (version 1.18.0) [4], resulting in normalized counts corrected for transcript length and sequencing depth, which we termed as base mean counts in our work. Subsequently, *FN1* transcripts were filtered. To obtain *FN1* transcripts that were robustly expressed, a cutoff was applied in the lesioned and preserved cartilage samples separately of an average of ≥ 10 counts per 3 samples.

Differential expression analysis and replication

Differential expression analysis was performed on the expressed *FN1* transcripts in 35 paired samples using the DESeq2 R package (version 1.30.1) [5]. A general linear model assuming a negative binomial distribution was applied, followed by a paired Wald's test comparing lesioned and preserved OA cartilage samples, with the preserved samples as the reference. P values less than 0.05 (after Benjamini-Hochberg correction) were considered significant and are reported as the false discovery rate (FDR). DEXSeq (version 1.36) was used to visualize the exon count data from *FN1* [6]. Moreover, replication of differentially expressed *FN1-208* was performed in an independent cohort of 10 paired cartilage samples (**Supplementary Table 1B**) as described previously [7]. Expression levels of *FN1-208* were measured with QuantStudio 6 Real-Time PCR system (Applied Biosystems) using FastStart SYBR Green Master reaction mix (Roche Applied Science). Relative gene expression levels (-ΔCt) were calculated using *GAPDH* as internal control, primer sequences are shown in **Supplementary Table 2**. A paired t-test was performed on the -ΔCt values, P values less than 0.05 were considered significant.

Lentiviral production and cell culture

Lentiviral production was performed in HEK293T cells using the Lenti-vpak Lentiviral Packaging kit (Origene Technologies) according to manufacturer's protocol. Virus particles were collected 48 and 72 hours post-transfection and stored at -80 °C. Virus titer was determined by p24 ELISA.

Primary chondrocytes were cultured as previously described [8]. For lentiviral transduction, cells were seeded at a cell density of $3.5x10^5$ cells per 10 cm culture dish. After one day in culture, cells were incubated for 16 hours with the corresponding lentivirus at multiplicity of infection (MOI) of 1 in the presence of 15 µg/ml Polybrene (Sigma-Aldrich), after which the medium was replaced with culture medium. After approximately 24 hours, medium was refreshed with culture medium with 0.5 µg/ml Puromycin (Sigma-Aldrich) to select for transduced cells. Cells were maintained in culture medium supplemented with Puromycin for 1 week,

subsequently the chondrocytes were expanded and *in vitro* chondrogenesis was induced as previously described [8]. Neo-cartilage pellets and medium were collected following three days of chondrogenesis. Surface area of the pellets was measured with CellSens Dimension (Olympus) software (version 3.1.1).

RNA isolation and relative gene expression analysis

For RNA isolation, two neo-cartilage pellets were pooled and lysed in 200 µl TRIzol reagent (Thermo Fisher Scientific) and homogenized using micro pestles. RNA was extracted with chloroform and purified from the supernatant using the RNeasy Mini kit (Qiagen). RNA concentration was measured using a Nanodrop-1000 photospectrometer (Thermo Scientific). Synthesis of cDNA was performed with 150 ng of total RNA using a First Strand cDNA Synthesis kit according to manufacturer's protocol (Roche Applied Science). The cDNA was diluted five times and pre-amplification with Taqman preamp master mix (Thermo Fisher Scientific) was performed for 16 genes of interest, primer sequences are shown in **Supplementary Table 2**. Expression levels were measured with QuantStudio 6 Real-Time PCR system using FastStart SYBR Green Master reaction mix. Relative gene expression levels (-ΔCt) were calculated using the average of Ct values of *GAPDH* and *SDHA* as internal controls. Fold changes were calculated with the $2^{-\Delta\Delta Ct}$ method. The ratio of specific *FN1* transcripts was calculated as follows: $\Delta Ct_{RATIO} = \Delta Ct_{TRANSCRIPT} - \Delta Ct_{FULL\ LENGTH\ FN1}$.

Histology and immunohistochemistry

Neo-cartilage pellets were fixed in 4% formaldehyde overnight and stored in 70% EtOH at 4 °C. They were then embedded in paraffin and sectioned at 5 µm. After sectioning, slides were deparaffinized and rehydrated. Sections were stained with 1% Alcian blue 8-GX (Sigma-Aldrich) and Nuclear Fast Red (Sigma-Aldrich) to visualize glycosaminoglycan deposition. To detect fibronectin (ab2413, Abcam, 1:400) immunohistochemistry was performed with 3-diaminobenzidine (DAB)-solution (Sigma-Aldrich) and hematoxylin (Klinipath) as described before [8]. Alcian blue staining was quantified by loading the images in Fiji (ImageJ version 2.1.0) [9] and splitting the color channels. Subsequently, grey values were measured of 3-5 separate squares per pellet and corrected for the grey value of the background.

References

1. Kim, D., et al., *Graph-based genome alignment and genotyping with HISAT2 and HISAT-genotype*. Nat Biotechnol, 2019. **37**(8): p. 907-915.
2. Patro, R., et al., *Salmon provides fast and bias-aware quantification of transcript expression*. Nat Methods, 2017. **14**(4): p. 417-419.
3. Cunningham, F., et al., *Ensembl 2019*. Nucleic acids research, 2019. **47**(D1): p. D745-D751.
4. Soneson, C., M.I. Love, and M.D. Robinson, *Differential analyses for RNA-seq: transcript-level estimates improve gene-level inferences*. F1000Res, 2015. **4**: p. 1521.
5. Love, M.I., W. Huber, and S. Anders, *Moderated estimation of fold change and dispersion for RNA-seq data with DESeq2*. Genome Biology, 2014. **15**(12).

6. Anders, S., A. Reyes, and W. Huber, *Detecting differential usage of exons from RNA-seq data*. Genome Res, 2012. **22**(10): p. 2008-17.
7. van Hoolwerff, M., et al., *Elucidating Epigenetic Regulation by Identifying Functional cis-Acting Long Noncoding RNAs and Their Targets in Osteoarthritic Articular Cartilage*. Arthritis Rheumatol, 2020. **72**(11): p. 1845-1854.
8. Bomer, N., et al., *Underlying molecular mechanisms of DIO2 susceptibility in symptomatic osteoarthritis*. Ann Rheum Dis, 2015. **74**(8): p. 1571-9.
9. Schneider, C.A., W.S. Rasband, and K.W. Eliceiri, *NIH Image to ImageJ: 25 years of image analysis*. Nat Methods, 2012. **9**(7): p. 671-5.

Supplementary Materials

Supplementary Tables

Supplementary Table 1 | Sample characteristics included in the (A) discovery, (B) replication, (C) transduction of primary chondrocytes with *FN1* targeting shRNA, and (D) correlation analyses.

A

Discovery						
Tissue type	**Mean age (range)**	**# Men**	**# Women**	**# Preserved**	**# Lesioned**	**# Total**
Knee	69.5 (48 -79)	14	42	28	28	56
Hip	64.4 (48 -79)	2	12	7	7	14
All	68.5 (48 -79)	16	54	35	35	70

B

Replication						
Tissue type	**Mean age (range)**	**# Men**	**# Women**	**# Preserved**	**# Lesioned**	**# Total**
Knee	64.6 (57 - 75)	3	2	5	5	10
Hip	68.2 (59 - 75)	2	3	5	5	10
All	66.4 (57 - 75)	5	5	10	10	20

C

Transduction shRNA targeting *FN1*				
Tissue type	**Mean age (range)**	**# Men**	**# Women**	**# Total**
Knee	68.2 (63-77)	3	3	6

D

Correlations						
Tissue type	**Mean age (range)**	**# Men**	**# Women**	**# Preserved**	**# Lesioned**	**# Total**
Knee	69.1 (46 - 79)	56	12	35	33	68
Hip	66.2 (48 - 82)	27	6	22	11	33
All	68.2 (46 - 82)	83	18	57	44	101

Supplementary Table 2 | Primer sequences to measure mRNA expression levels

Gene	Forward primer (5' --> 3')	Reverse primer (5' --> 3')
ACAN	AGAGACTCACACAGTCGAAACAGC	CTATGTTACAGTGCTCGCCAGTG
ADAMTS-5	GTGGTGAAGGTGGTGGTGCT	CTCATGGTCATCTCCCAGCTG
ANKH	GTCTGCATGGCTCTGTCACT	AGGCAAAGTCCACTCCGATG
COL1A1	GTGCTAAAGGTGCCAATGGT	ACCAGGTTCACCGCTGTTAC
COL2A1	CTACCCCAATCCAGCAAACGT	AGGTGATGTTCTGGGAGCCTT
FN1 full length	GGATGGGGAGCAGAGTTTGA	GGTGTCATCAACTTGGTCCAC
FN1-208	AATGCACCACAGCCATCTCA	AGGTTTCTGGGTGGGATACTC
GAPDH	TGCCATGTAGACCCCTTGAAG	ATGGTACATGACAAGGTGCGG
ITGA5	GTCGGGGGCTTCAACTTAGAC	AGCACACTGACCCCGTCTG
ITGAV	TCTCTCGGGACTCCTGCTAC	AAGAAACATCCGGGAAGACGC
ITGB1	AGCGAAGGCATCCCTGAAAG	AATGTCTACCAACACGCCCT
ITGB5	CAGCAGCTTCCATGTCCTGA	AGGTTCACGGCAATCTCCTG
MMP-3	GAGGCATCCACACCCTAGGTT	TCAGAAATGGCTGCATCGATT
MMP-13	TTGAGCTGGACTCATTGTCG	GGAGCCTCTCAGTCATGGAG
NT5E	ATTGCACTGGGACATTCGGG	TGGAAGGTGGATTGCCTGTG
RUNX2	CAATTTCCTCCTTGCCCCTCA	TCGGATCTACGGGAATACGCA
SDHA	TGGGAACAAGAGGGCATCTG	GCCTACCACCACTGCATCAA
SOX9	CCCCAACAGATCGCCTACAG	CTGGAGTTCTGGTGGTCGGT
TNFRS11B	TTGATGGAAAGCTTACCGGGA	TCTGGTCACTGGGTTTGCATG

Supplementary Table 3 | False discovery rate significantly differentially expressed *FN1* transcripts in lesioned versus preserved OA cartilage in knee samples.

Ensembl ID	Name	Biotype	baseMean	FoldChange	Pvalue	Padj
ENST00000480024.1	FN1-220	Retained intron	277.2	2.76	2.64E-14	5.80E-13
ENST00000494446.1	FN1-225	Retained intron	33536.1	2.44	3.98E-09	4.38E-08
ENST00000473614.1	FN1-218	Retained intron	155.2	2.30	2.28E-08	1.67E-07
ENST00000492816.6	FN1-224	Retained intron	2028.0	2.38	6.03E-07	3.31E-06
ENST00000426059.1	FN1-208	Protein coding	16523.2	2.35	1.10E-06	4.86E-06
ENST00000496542.1	FN1-226	Retained intron	87.6	2.88	1.49E-06	5.45E-06
ENST00000421182.5	FN1-207	Protein coding	30469.0	2.57	1.72E-04	5.39E-04
ENST00000490833.5	FN1-223	Processed transcript	8.8	2.30	3.91E-04	1.08E-03
ENST00000460217.1	FN1-214	Retained intron	447.5	1.76	8.85E-04	2.09E-03
ENST00000471193.1	FN1-217	Retained intron	903.3	2.21	9.49E-04	2.09E-03
ENST00000498719.1	FN1-227	Retained intron	50673.0	2.30	2.62E-03	5.23E-03
ENST00000469569.1	FN1-216	Retained intron	41.5	1.70	8.08E-03	1.48E-02
ENST00000461974.1	FN1-215	Retained intron	2163.2	1.80	9.75E-03	1.65E-02
ENST00000446046.5	FN1-212	Protein coding	37427.2	2.11	1.90E-02	2.99E-02
ENST00000356005.8	FN1-204	Protein coding	112854.7	2.14	3.59E-02	4.99E-02
ENST00000432072.6	FN1-209	Protein coding	234116.5	1.96	3.63E-02	4.99E-02

baseMean = mean of normalized counts of all samples normalized for transcript length and sequencing depth, FoldChange = fold change between lesioned and preserved OA cartilage samples, Pvalue = nominal P value, Padj = P value according to false discovery rate.

Supplementary Table 4 | Significantly differentially expressed *FN1* transcripts in lesioned versus preserved osteoarthritic cartilage in hip samples.

Ensembl ID	Name	Biotype	baseMean	FoldChange	Pvalue	Padj
ENST00000480024.1	FN1-220	Retained intron	277.2	2.76	2.64E-14	5.01E-13
ENST00000494446.1	FN1-225	Retained intron	33536.1	2.44	3.98E-09	3.78E-08
ENST00000473614.1	FN1-218	Retained intron	155.2	2.30	2.28E-08	1.45E-07
ENST00000492816.6	FN1-224	Retained intron	2028	2.38	6.03E-07	2.86E-06
ENST00000426059.1	FN1-208	Protein coding	16523.2	2.35	1.10E-06	4.19E-06
ENST00000496542.1	FN1-226	Retained intron	87.6	2.88	1.49E-06	4.71E-06
ENST00000421182.5	FN1-207	Protein coding	30469	2.57	1.72E-04	4.66E-04
ENST00000460217.1	FN1-214	Retained intron	447.5	1.76	8.85E-04	2.00E-03
ENST00000471193.1	FN1-217	Retained intron	903.3	2.21	9.49E-04	2.00E-03
ENST00000498719.1	FN1-227	Retained intron	50673	2.30	2.62E-03	4.97E-03
ENST00000469569.1	FN1-216	Retained intron	41.5	1.70	8.08E-03	1.40E-02
ENST00000461974.1	FN1-215	Retained intron	2163.2	1.80	9.75E-03	1.54E-02
ENST00000446046.5	FN1-212	Protein coding	37427.2	2.11	1.90E-02	2.78E-02
ENST00000356005.8	FN1-204	Protein coding	112854.7	2.14	3.59E-02	4.60E-02
ENST00000432072.6	FN1-209	Protein coding	234116.5	1.96	3.63E-02	4.60E-02
ENST00000357867.8	FN1-205	Protein coding	23405.6	0.44	3.96E-02	4.71E-02

baseMean = mean of normalized counts of all samples normalized for transcript length and sequencing depth, FoldChange = fold change between lesioned and preserved OA cartilage samples, Pvalue = nominal P value, Padj = P value according to false discovery rate.

Supplementary Table 5 | Effect of modulating *FN1* and relative *FN1-208* expression on cartilage relevant genes in pellets from primary chondrocytes transduced with non-targeting (control) and *FN1* targeting shRNA after 3 days of chondrogenesis. P values were determined by generalized estimation equations, with experimental read-out as dependent variable and donor and group as covariate.

Gene	Fold change	P value
ACAN	0.5	5.7E-03
ADAMTS-5	2.6	9.0E-06
ANKH	1.5	1.4E-01
COL1A1	0.7	3.2E-01
COL2A1	0.1	7.0E-07
FN1 full length	0.3	7.6E-07
FN1-208	3.5	6.0E-06
ITGA5	1.1	8.0E-01
ITGAV	0.9	4.8E-01
ITGB1	1.9	4.0E-06
ITGB5	2.1	1.2E-03
MMP-3	0.4	2.9E-02
MMP-13	0.3	3.2E-02
NT5E	2.5	3.0E-06
RUNX2	0.6	6.2E-02
SOX9	0.8	2.2E-01
TNFRS11B	1.0	9.5E-01

Supplementary Table 6 | Correlations > |0.7| between significant differently expressed genes and *FN1* in the same lesioned and preserved osteoarthritic cartilage samples.

Ensembl ID	Gene	FoldChange	Cor	Pval
ENSG00000151150	ANK3	2.62	0.87	2.22E-16
ENSG00000150764	DIXDC1	1.53	0.86	2.22E-16
ENSG00000116991	SIPA1L2	1.78	0.84	2.22E-16
ENSG00000164761	TNFRSF11B	3.01	0.84	2.22E-16
ENSG00000139514	SLC7A1	1.44	0.83	2.22E-16
ENSG00000154122	ANKH	1.44	0.82	2.22E-16
ENSG00000163399	ATP1A1	1.29	0.82	2.22E-16
ENSG00000135318	NT5E	2.00	0.81	2.22E-16
ENSG00000146352	CLVS2	2.15	0.81	2.22E-16
ENSG00000173698	ADGRG2	1.59	0.80	2.22E-16
ENSG00000185634	SHC4	2.10	0.78	2.22E-16
ENSG00000158966	CACHD1	1.80	0.78	2.22E-16
ENSG00000173276	ZBTB21	1.36	0.78	2.22E-16
ENSG00000282121	AL592430.2	1.95	0.77	2.22E-16
ENSG00000154229	PRKCA	1.24	0.77	2.22E-16
ENSG00000173267	SNCG	0.61	-0.77	2.22E-16
ENSG00000137070	IL11RA	0.80	-0.76	2.22E-16
ENSG00000168675	LDLRAD4	1.33	0.76	2.22E-16
ENSG00000188706	ZDHHC9	1.24	0.76	2.22E-16
ENSG00000204592	HLA-E	0.72	-0.76	2.22E-16
ENSG00000167994	RAB3IL1	0.48	-0.76	2.22E-16
ENSG00000211455	STK38L	1.65	0.76	2.22E-16
ENSG00000235750	KIAA0040	1.50	0.76	2.22E-16
ENSG00000118596	SLC16A7	1.61	0.75	2.22E-16
ENSG00000204291	COL15A1	1.74	0.74	2.22E-16
ENSG00000144648	ACKR2	1.80	0.74	2.22E-16
ENSG00000147642	SYBU	1.26	0.74	2.22E-16
ENSG00000244486	SCARF2	0.62	-0.74	2.22E-16
ENSG00000156535	CD109	1.54	0.74	2.22E-16
ENSG00000154721	JAM2	0.61	-0.74	2.22E-16
ENSG00000134198	TSPAN2	2.42	0.73	2.22E-16
ENSG00000182934	SRPRA	1.14	0.73	2.22E-16
ENSG00000161638	ITGA5	1.45	0.73	2.22E-16
ENSG00000123933	MXD4	0.78	-0.73	2.22E-16
ENSG00000241839	PLEKHO2	0.70	-0.73	2.22E-16
ENSG00000187957	DNER	3.37	0.73	2.22E-16
ENSG00000151693	ASAP2	1.34	0.72	2.22E-16
ENSG00000135269	TES	1.35	0.72	2.22E-16
ENSG00000196305	IARS	1.32	0.72	2.22E-16
ENSG00000185386	MAPK11	0.74	-0.72	2.22E-16
ENSG00000153823	PID1	1.48	0.72	2.22E-16
ENSG00000185760	KCNQ5	1.32	0.72	2.22E-16
ENSG00000134243	SORT1	1.40	0.72	2.22E-16
ENSG00000178752	ERFE	3.44	0.72	2.22E-16
ENSG00000150995	ITPR1	1.58	0.72	2.22E-16
ENSG00000171621	SPSB1	1.57	0.71	2.22E-16
ENSG00000182580	EPHB3	0.52	-0.71	2.22E-16
ENSG00000134802	SLC43A3	0.66	-0.71	2.22E-16
ENSG00000117020	AKT3	1.43	0.71	2.22E-16

Ensembl ID	Gene	FoldChange	Cor	Pval
ENSG00000154930	ACSS1	0.51	-0.71	2.22E-16
ENSG00000182752	PAPPA	3.43	0.71	2.22E-16
ENSG00000141441	GAREM1	1.30	0.71	2.22E-16
ENSG00000150907	FOXO1	1.22	0.71	2.22E-16
ENSG00000196352	CD55	2.96	0.71	2.22E-16
ENSG00000152503	TRIM36	2.85	0.71	2.22E-16
ENSG00000140526	ABHD2	1.49	0.70	2.22E-16
ENSG00000132334	PTPRE	1.30	0.70	4.44E-16
ENSG00000197892	KIF13B	1.37	0.70	4.44E-16
ENSG00000187244	BCAM	0.64	-0.70	4.44E-16
ENSG00000165434	PGM2L1	1.88	0.70	4.44E-16

FoldChange = fold change between lesioned and preserved OA cartilage samples, Cor = correlation, Pval = nominal P value

Supplementary Table 7 | False discovery rate (FDR) significantly enriched Gene Ontology processes between highly correlated genes (|r| > 0.7) and *FN1* analyzed using STRING.

Term ID	Term description	Observed gene count	Background gene count	FDR	Matching proteins in network
GO:0009986	Cell surface	12	824	0.012	SORT1, NT5E, BCAM, ANK3, CD109, ITGA5, CD55, HLA-E, GPR64, JAM2, ACKR2, IL11RA
GO:0005886	Plasma membrane	31	5314	0.043	PTPRE, SORT1, NT5E, SLC16A7, ABHD2, GAREM, BCAM, ANK3, ASAP2, ANKH, CD109, CACHD1, ITGA5, TNFRSF11B, ITPR1, SHC4, EPHB3, KCNQ5, DNER, FN1, TES, CD55, TSPAN2, HLA-E, GPR64, SLC7A1, JAM2, PRKCA, ACKR2, ATP1A1, IL11RA
GO:0016020	Membrane	43	9072	0.043	PTPRE, SORT1, NT5E, SLC16A7, AKT3, ABHD2, GAREM, BCAM, CLVS2, ANK3, ASAP2, ANKH, CD109, CACHD1, ITGA5, TNFRSF11B, ITPR1, SRPR, SHC4, EPHB3, KCNQ5, DNER, FN1, ZDHHC9, TES, LDLRAD4, CD55, TSPAN2, COL15A1, IARS, HLA-E, GPR64, SLC7A1, STK38L, JAM2, SYBU, PRKCA, ACKR2, SLC43A3, ATP1A1, IL11RA, KIAA0040, SCARF2
GO:0031982	Vesicle	25	3879	0.043	SORT1, NT5E, ABHD2, BCAM, CLVS2, TRIM36, CD109, ITGA5, ITPR1, PLEKHO2, SRPR, DNER, FN1, LDLRAD4, CD55, SNCG, COL15A1, IARS, HLA-E, GPR64, RAB3IL1, SYBU, PRKCA, ACKR2, ATP1A1
GO:0031224	Intrinsic component of membrane	30	5345	0.046	PTPRE, SORT1, NT5E, SLC16A7, ABHD2, BCAM, ANKH, CD109, CACHD1, ITGA5, ITPR1, EPHB3, KCNQ5, DNER, ZDHHC9, LDLRAD4, CD55, TSPAN2, COL15A1 ,HLA-E, GPR64, SLC7A1, JAM2, SYBU, ACKR2, SLC43A3, ATP1A1, IL11RA, KIAA0040, SCARF2

Supplementary Figures

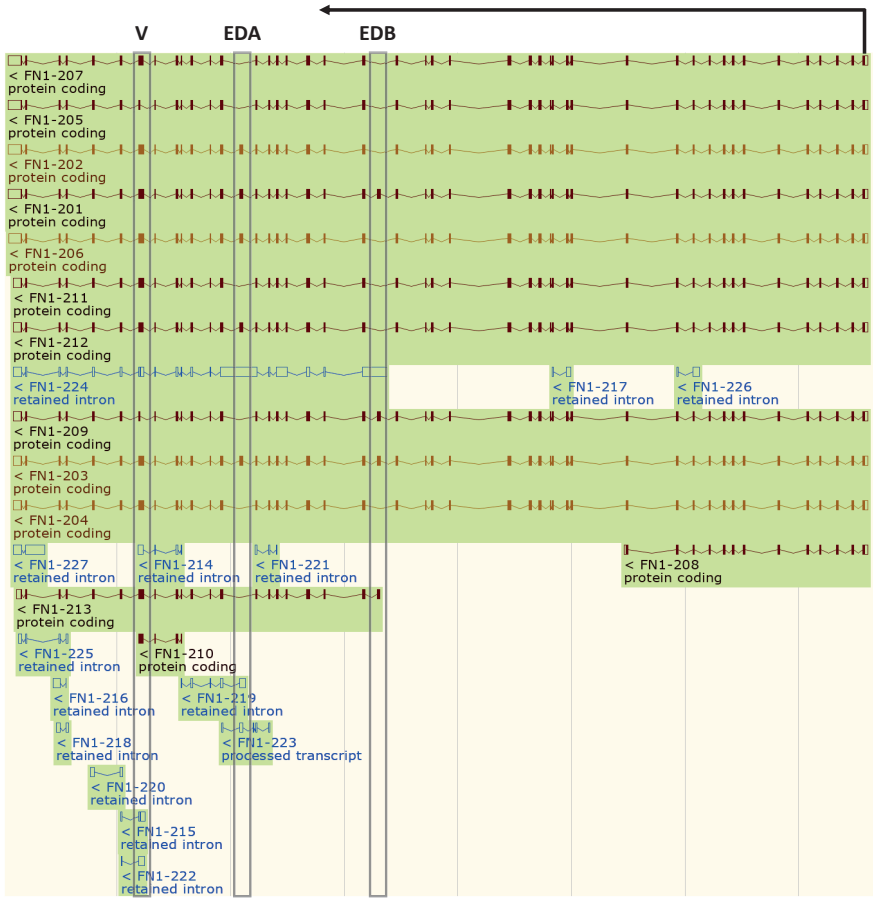

Supplementary Figure 1 | Overview of *FN1* transcripts as annotated in the Ensembl database, which are transcribed from the antisense strand, represented by the black arrow. The black squares represent the three regions of alternative splicing, from 5' to 3' the Extra Domain B (EDB), Extra domain A (EDA), and Variable region (V). Source: https://www.ensembl.org/index.html

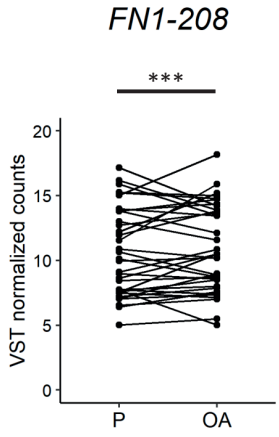

Supplementary Figure 2 | *FN1-208* was significantly upregulated (FC = 2.3) in lesioned (OA) versus preserved (P) osteoarthritic cartilage samples as determined by RNA-sequencing in 35 paired cartilage samples. *** P value according to false discovery rate < 0.001.

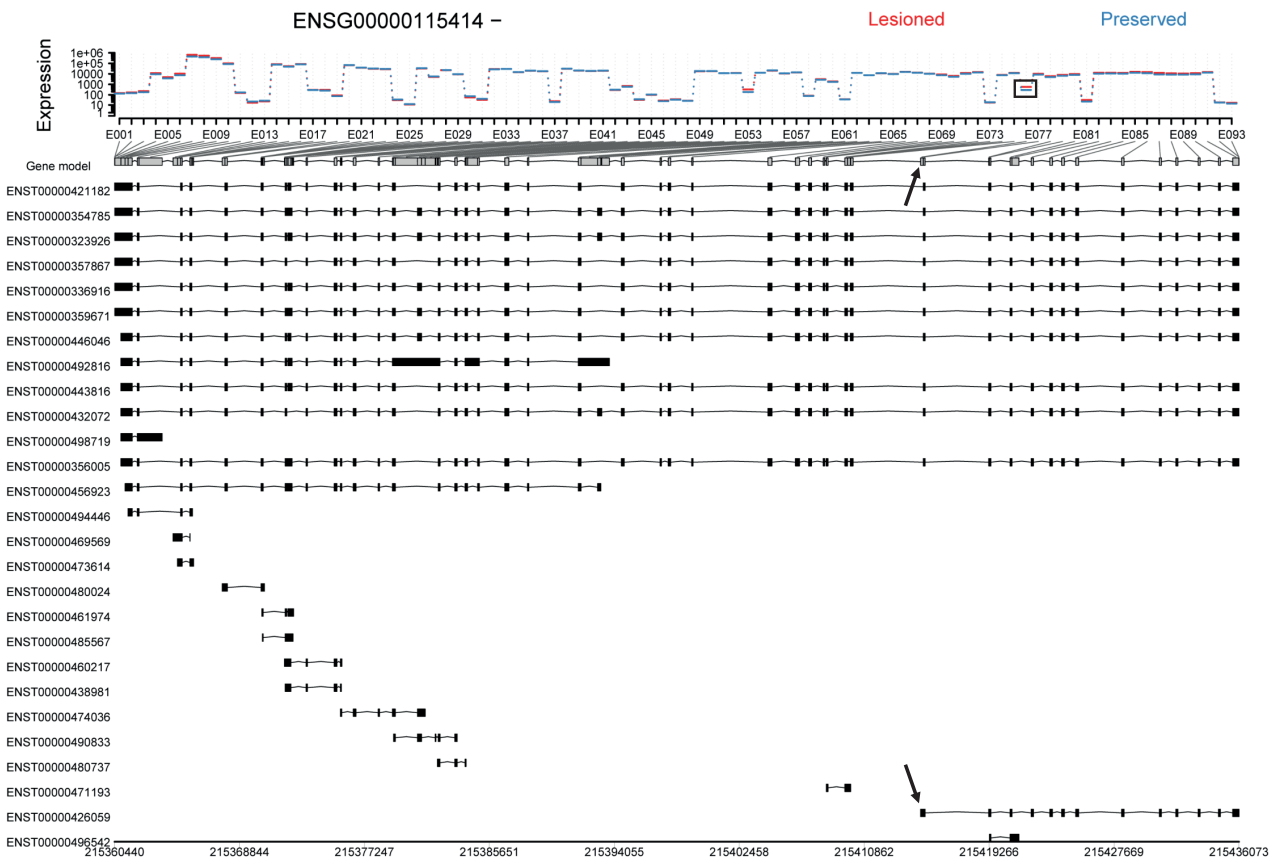

Supplementary Figure 3 | Overview of exon count data of all *FN1* transcripts in lesioned versus preserved OA cartilage. The exons are divided into bins that are identical across all transcripts. The most prominent difference between lesioned and preserved is the bin marked by the black box, which corresponds to the bin marked by the black arrows, which is the specific exon that is unique for *FN1-208* (ENST00000426059 in figure).

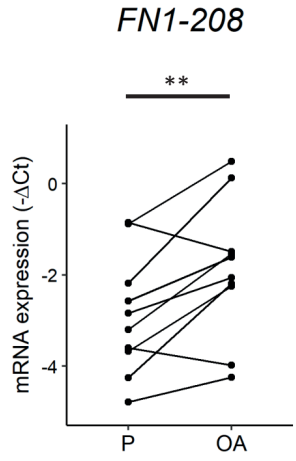

Supplementary Figure 4 | Replication of *FN1-208* upregulation (FC = 2.0) in lesioned (OA) and preserved (P) osteoarthritic cartilage samples by RT-qPCR in 10 independent paired samples. ** P < 0.01, as determined by paired t-test on -ΔCt values per donor.

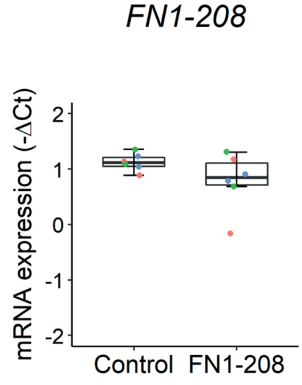

Supplementary Figure 5 | Unsuccessful overexpression of *FN1-208* in neo-cartilage pellets of primary chondrocytes of 3 donors transduced with pLV-CMV-eGFP-FN1-208 (FN1-208) compared to cells transduced with empty vector pLV-CMV-eGFP (control). Individual samples are represented by colored dots, colors of the dots represent different donors.